Effects of injected ice particles in the lower stratosphere on the Antarctic ozone hole

H. Nagase[1,2], D. E. Kinnison[3], A. K. Petersen[2], F. Vitt[3], and G. P. Brasseur[2,3]

[1]Graduate School of Pharmaceutical Sciences, Osaka University, Osaka, Japan, [2]Max Planck Institute for Meteorology, Hamburg, Germany, [3]National Center for Atmospheric Research, Boulder, Colorado, USA

Abstract The Antarctic ozone hole will continue to be observed in the next 35–50 years, although the emissions of chlorofluorocarbons (CFCs) have gradually been phased out during the last two decades. In this paper, we suggest a geo-engineering approach that will remove substantial amounts of hydrogen chloride (HCl) from the lower stratosphere in fall, and hence limit the formation of the Antarctic ozone hole in late winter and early spring. HCl will be removed by ice from the atmosphere at temperatures higher than the threshold under which polar stratospheric clouds (PSCs) are formed if sufficiently large amounts of ice are supplied to produce water saturation. A detailed chemical-climate numerical model is used to assess the expected efficiency of the proposed geo-engineering method, and specifically to calculate the removal of HCl by ice particles. The size of ice particles appears to be a key parameter: larger particles (with a radius between 10 and 100 μm) appear to be most efficient for removing HCl. Sensitivity studies lead to the conclusions that the ozone recovery is effective when ice particles are supplied during May and June in the latitude band ranging from 70°S to 90°S and in the altitude layer ranging from 10 to 26 km. It appears, therefore, that supplying ice particles to the Antarctic lower stratosphere could be effective in reducing the depth of the ozone hole. In addition, photodegradation of CFCs might be accelerated when ice is supplied due to enhanced vertical transport of this efficient greenhouse gas.

1. Introduction

The release of industrially manufactured halocarbons into the atmosphere since the 1950s has led to gradual depletion of stratospheric ozone with the unexpected appearance in the 1980s of a large springtime ozone hole in Antarctica [*Chubachi*, 1984; *Farman et al.*, 1985; *World Meteorological Organization* (*WMO*), 2007]. In response to the Montreal Protocol on Substances that Deplete the Ozone Layer (1987), measures have been taken to gradually phase out the emissions of the most detrimental chlorofluorocarbons (CFCs). As a result, the level of stratospheric inorganic chlorine has started to decrease and will further do so in the future decades [*WMO*, 2007]. However, due to the long atmospheric lifetime of halocarbons, it is expected that the ozone hole will continue to be observed in the next 35–50 years [*Eyring et al.*, 2010].

Ozone depletion increases the intensity of UV-B, which produces harmful effects on the biological life [*United Nations Environment Programme* (*UNEP*), 2010]. Among the biological effects are skin and eye diseases [*UNEP*, 2010]. One of the most serious problems is the potential decline of phytoplankton and zooplankton in the Antarctic Ocean [*Naganobu et al.*, 1999; *Boyce et al.*, 2010; *UNEP*, 2010], with adverse impacts on the food chain.

Hydrogen chloride (HCl) is the most abundant inorganic chlorine reservoir in the stratosphere. If converted into reactive chlorine (Cl, ClO) by heterogeneous activation on the surface of liquid or solid particles in polar stratospheric clouds (PSCs), it causes rapid ozone depletion and leads to the formation of the ozone hole [*Solomon et al.*, 1986; *Solomon*, 1988; *WMO*, 1989, 1991; *Brasseur and Solomon*, 2005]. The ozone destruction in Antarctica could, however, be significantly reduced if one could establish a systematic method that would reduce the stratospheric concentration of HCl prior to the chlorine activation period by PSCs.

Here, we suggest a geo-engineering approach by which large quantities of HCl could be removed from the polar lower stratosphere. The method consists of injecting ice at about 25 km altitude in late austral fall before chlorine is activated by the presence of PSC particles. During fall, the temperature is generally higher than the threshold under which type I and type II PSCs are produced (195 and 187 K, respectively). When

a large amount of water at partial pressure above the saturation vapor pressure of ice is injected as water vapor or ice around 25 km altitude, it is expected to remain as ice particles for several days. Because HCl dissolves in ice particles, and because these particles, if sufficiently large, gravitationally sediment, substantial amounts of chlorine can be removed from the polar stratosphere through this mechanism. The paper briefly reviews the uptake of gas-phase HCl by ice particles with emphasis on the calculation of the uptake coefficients. It presents numerical simulations of the Antarctic ozone hole, using the Whole Atmosphere Community Climate Model (WACCM), and assesses, on the basis of these model simulations, the response of ozone to the injection of ice particles in the polar lower stratosphere. This study should be viewed as an initial first-order investigation aimed at developing a concept rather than providing final quantitative values. The analysis should be completed in the future by more detailed simulations that analyze, in more detail, the important feedbacks on atmospheric circulation and the possible impacts to the climate system.

2. Description of the Uptake Coefficient

Chlorine is activated on the surface of PSC particles, and is converted mostly into gas-phase Cl_2. Major heterogeneous reactions on ice particles are

$$ClONO_2\,(g) +\ HCl\,(ads)\ \rightarrow\ Cl_2\,(g) +\ HNO_3\,(ads) \tag{R1}$$

$$ClONO_2\,(ads) +\ H_2O\,(surf)\ \rightarrow\ HOCl\,(g) +\ HNO_3\,(ads) \tag{R2}$$

$$HOCl\,(g) +\ HCl\,(ads) \rightarrow\ Cl_2\,(g) +\ H_2O\,(surf) \tag{R3}$$
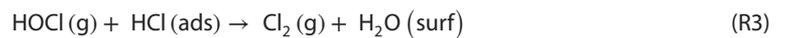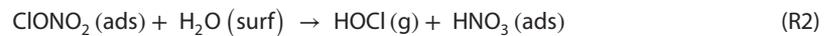
where g, ads, and surf denote gas-phase, adsorbed, and surface, respectively. Heterogeneous reactions R1 and R3 are known as an Eley-Ridel (ER) type mechanism [*Fernandez et al.*, 2005; *McNeill et al.*, 2007; *Crowley et al.*, 2010; *Hynes et al.*, 2001]: gas-phase species, $ClONO_2$(g) and HOCl(g), directly react with HCl(ads) at the surface of ice particles. Heterogeneous reaction R2 is known as a Langmuir-Hinshelwood (LH) type mechanism [*Fernandez et al.*, 2005]: gas-phase $ClONO_2$ adsorbed on ice surface reacts with H_2O(surf).

The rate of gas loss due to heterogeneous processes can be represented by an uptake coefficient, γ_X, which is the net probability that a molecule X undergoing a gas-kinetic collision with a surface is actually taken up by the surface [*Crowley et al.*, 2010],

$$-\,d\,[X]_g\,/dt =\ k\,[X]_g = \gamma_X \overline{v}_X A\,[X]_g\,/4 \tag{1}$$

Here, $[X]_g$ is the concentration of X in the gas phase (molecule/cm^3), k is the first-order rate coefficient for loss (1/s), $\overline{v}_X$ is the mean thermal velocity of X ($\overline{v}_X = \sqrt{8k_B T/m_X \pi}$ (cm/s)), and A is the specific surface area density of condensed phase in a given volume of air (cm^2/cm^3). The uptake kinetics of gas into PSCs depends on gas-phase diffusion, mass accommodation, Henry's law solubility, and chemical reaction in the aqueous bulk phase or at the gas–liquid interface. Therefore, the total uptake coefficient for each species, γ_X, is expressed by

$$\frac{1}{\gamma_{ClONO2}} =\ \frac{1}{\Gamma_g^{ClONO2}} + \frac{1}{\Gamma_{R1}^{ClONO2} + \Gamma_{R2}^{ClONO2}} \tag{2}$$

$$\frac{1}{\gamma_{HOCl}} =\ \frac{1}{\Gamma_g^{HOCl}} + \frac{1}{\Gamma_{R3}^{HOCl}} \tag{3}$$

$$\frac{1}{\gamma_{HCl}} =\ \frac{1}{\Gamma_g^{HCl}} + \frac{1}{\alpha_{HCl}} + \frac{1}{\Gamma_{R1}^{HCl} + \Gamma_{R3}^{HCl} + \Gamma_{sol}^{HCl}} \tag{4}$$

where Γ_g^x is the uptake coefficient for gas-phase, α_x the surface accommodation coefficient, Γ_{Ri}^x the uptake coefficient for each reaction, and Γ_{sol}^x the uptake coefficient for dissolution.

In the earlier studies based on WACCM, the effects of Γ_g^x and Γ_{sol}^x were ignored, and Γ_{R1}^{ClONO2}, Γ_{R2}^{ClONO2}, and Γ_{R3}^{HOCl} were assumed to be constant at 0.3, 0.3, and 0.2, respectively. However, it is necessary to consider these parameters in more detail, when large amounts of ice are supplied and sedimented at relatively high

rate. Coefficient Γ_g^X is dependent on the particle's radius a and the terminal velocity U of ice particles. It is expressed as

$$\Gamma_g^X = 2D_g^X Sh_X / a\bar{v}_X \tag{5}$$

where D_g^X is the binary diffusion coefficient for gases, X and air, $\bar{v}_X$ is the mean thermal velocity of X, and Sh_X is the Sherwood number, which is a function of U. These parameters are expressed in Table A1.

The expression for Γ_{Ri}^X depends on the reaction type. In the case of the ER type mechanism (R1 and R3), gas phase $ClONO_2$ and HOCl directly react with surface HCl. Therefore, parameters Γ_{R1}^{ClONO2} and Γ_{R3}^{HOCl} can be expressed by [*Fernandez et al.*, 2005; *Crowley et al.*, 2010]

$$\Gamma_{R1}^{ClONO2} = \gamma_{gs}^{ClONO2} \theta_{HCl} \tag{6}$$

$$\Gamma_{R3}^{HOCl} = \gamma_{gs}^{HOCl} \theta_{HCl} \tag{7}$$

where γ_{gs}^X is the elementary gas-surface reactive uptake coefficient and θ_{HCl} is the fractional surface coverage of HCl on ice. Γ_{R2}^{ClONO2}, which refers to a LH type mechanism [*Fernandez et al.*, 2005], is expressed by

$$\frac{1}{\Gamma_{R2}^{ClONO2}} = \frac{1}{\alpha_{ClONO2}} + \frac{\bar{v}_{ClONO2}\left(1 + K_{lang}^{ClONO2}[ClONO_2]_g\right)}{4k_s[H_2O]_s K_{lang}^{ClONO2} N_{max}^{ClONO2}} \tag{8}$$

The parameters used in Equations (6)–(8) are expressed in Table A2.

In the case of HCl, heterogeneous reactions R1 and R3 are related. First, the reaction rate of the heterogeneous reaction R1 is expressed by

$$-d[ClONO_2]_g/dt = \Gamma_{R1,\,net}^{ClONO2}\bar{v}_{ClONO2}A[ClONO_2]_g/4 \tag{9}$$

$$-Ad[HCl]_{ads}/dt = \Gamma_{R1}^{HCl}\bar{v}_{HCl}A[HCl]_g/4 \tag{10}$$

If one assumes that the dominant activation process is provided by reaction R1, the rate of $ClONO_2$ and HCl destruction should be approximately equal, and by comparing Equations (9) and (10), one obtains

$$\Gamma_{R1}^{HCl} = \Gamma_{R1,\,net}^{ClONO2}\frac{\bar{v}_{ClONO2}[ClONO_2]_g}{\bar{v}_{HCl}[HCl]_g} \tag{11}$$

Because $ClONO_2$ is consumed simultaneously by heterogeneous reactions R1 and R2, $\Gamma_{R1,\,net}^{ClONO2}$ is expressed as

$$\Gamma_{R1,\,net}^{ClONO2} = \gamma_{ClONO2}\frac{\Gamma_{R1}^{ClONO2}}{\Gamma_{R1}^{ClONO2} + \Gamma_{R2}^{ClONO2}} \tag{12}$$

By combining Equations (11) and (12), the expression for Γ_{R1}^{HCl} becomes

$$\Gamma_{R1}^{HCl} = \gamma_{ClONO2}\frac{\Gamma_{R1}^{ClONO2}}{\Gamma_{R1}^{ClONO2} + \Gamma_{R2}^{ClONO2}}\frac{\bar{v}_{ClONO2}[ClONO_2]_g}{\bar{v}_{HCl}[HCl]_g} \tag{13}$$

Similarly, Γ_{R3}^{HCl} is expressed by considering heterogeneous reaction R3

$$\Gamma_{R3}^{HCl} = \gamma_{HOCl}\frac{\bar{v}_{HOCl}[HOCl]_g}{\bar{v}_{HCl}[HCl]_g} \tag{14}$$

The diffusive uptake of HCl into the bulk of the ice is dependent on the exposure time of ice to HCl, Δt. Therefore, Γ_{sol}^{HCl} is expressed as [*Vesala et al.*, 2001; *Sander et al.*, 2011]

$$\Gamma_{sol}^{HCl} = \frac{8H_d^{HCl}}{\bar{v}_{HCl}}\sqrt{\frac{D_{ice}^{HCl}}{\pi\Delta t}} \tag{15}$$

where D_{ice}^{HCl} is the bulk phase diffusion coefficient for HCl in ice. A range of 10^{-17} to 10^{-15} m^2/s has been reported for the value of this quantity [*Aguzzi et al.*, 2003; *Huthwelker et al.*, 2004; *Cox et al.*, 2005] under stratospheric conditions. *Huthwelker et al.* [2004] mentioned that the value of 10^{-16} m^2/s for D_{ice}^{HCl} seems a reasonable upper limit. The parameter H_d^{HCl} denotes the dimensionless Henry's constant for HCl in ice with a wide range of values reported in the literature [*Seinfeld and Pandis*, 2006; *Krieger et al.*, 2002; *Huthwelker et al.*, 2004]. The value of 10^1 m/s$^{1/2}$ for $H_d^{HCl} D_{ice}^{HCl\ 1/2}$, obtained experimentally around 200 K at the stratospheric HCl concentration [*Huthwelker et al.*, 2004], was adopted in this study.

3. Model Simulations

3.1. Model Description

To simulate the response of stratospheric ozone to the proposed geo-engineering mechanism, we adopt the National Center for Atmospheric Research (NCAR) Whole Atmosphere Community Climate Model, version 4 (WACCM4) [*Marsh et al.*, 2013], in which the mechanism for heterogeneous chemistry has been updated on the basis of the discussion presented in the previous section. WACCM4 can be implemented in two different modes: (1) a free-running (FR) mode with fully interactive calculations of the chemical composition, temperature, and dynamics, based on the finite volume dynamical core [*Lin*, 2004] of the NCAR Community Atmosphere Model (CAM) [*Neale et al.*, 2013; *Marsh et al.*, 2013] and (2) a specified dynamics (SD) mode in which GEOS 5.1 (Goddard Earth Observing System) data from NASA are nudged into the model [*Kunz et al.*, 2011; *Lamarque et al.*, 2012]. This latter case, with limited interactive processes included, is expected to provide more realistic meteorological situations so that the results for a specified time period can be more easily compared with observations. In this study, the SD-WACCM simulations were performed for the period 1 January 2005 to 31 December 2005. The corresponding model results were compared with their FR model counterparts (FR-WACCM). The chemical module of WACCM4 is based upon the 3-D chemical transport Model of OZone and Related Tracers, version 3 [MOZART, *Kinnison et al.*, 2007]. It includes a detailed representation of the chemical and physical processes from the troposphere through the lower thermosphere. The species included within this mechanism are contained within the O_X, NO_X, HO_X, ClO_X, and BrO_X chemical families, along with CH_4 and its degradation products. In addition, fourteen primary non-methane hydrocarbons and related oxygenated organic compounds are included [*Emmons et al.*, 2010]. This mechanism contains 122 species, 218 gas-phase reactions, 74 photolytic processes, and 17 heterogeneous reactions on multiple aerosol types. The horizontal resolution is $1.9° \times 2.5°$ (latitude $\times$ longitude), with 66 and 88 pressure levels in the vertical from the surface to about 150 km altitude for FR and SD, respectively. In a recent validation effort, the interactive version of WACCM was shown to perform very well in comparison with many other chemistry-climate models [*SPARC CCMVal*, 2010].

Some small adjustments were made to the model to improve the formulation of polar processes. First, the parameterizations of gas phase diffusion, heterogeneous reaction, and uptake of HCl by ice particles were improved as mentioned in Section 2. Second, the representation of mixed PSCs (Nitric Acid Trihydrate (NAT) and Supercooled Ternary Solutions (STS) droplets) was updated based on the method recently reported by *Wegner et al.* [2013]; the uptake of HCl into STS was also added in the model [*Carslaw et al.*, 1995]. Third, the calculation of dehydration was slightly modified: In the earlier version of CAM, dehydration occurs above 80% saturation, which causes over-dehydration in the polar regions. The present model version adopts a value that is more in line with laboratory data, and assumes that dehydration starts at 100% saturation poleward of 60° and lower than 300 hPa.

3.2. Baseline Model Results by SD-WACCM

In order to constrain our analysis to a simplified situation, we first considered the results based on SD-WACCM, in which the temperature and dynamics are externally specified (data in 2005 was nudged, see above). A first simulation was performed with the model without supplying ice to the lower stratosphere (SD-control case). The volume mixing ratio of several chemical species around 85°S latitude and at 20 km of altitude is shown in Figures 1a and 1d. In late May, the temperature becomes lower than the threshold under which PSCs are formed. Gradually, the mixing ratio of ClONO$_2$ decreases from 0.5 ppbv in April and reaches almost zero in June. During the same period, the concentration of HCl is considerably reduced from 1.5 ppbv in April to 0.9 ppbv in June (Figure 1a). Chlorine is activated on the surface of PSC particles,
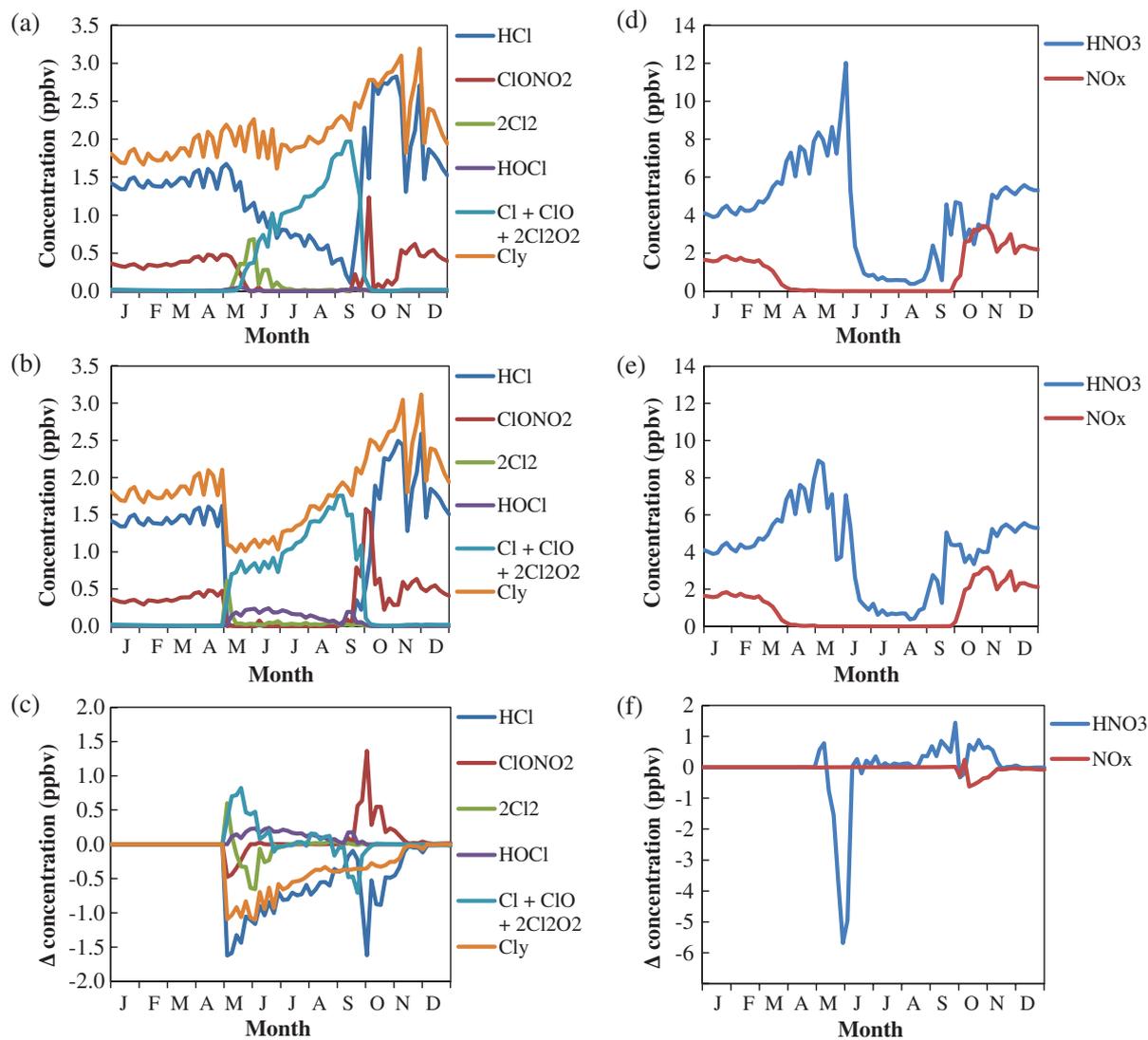
Figure 1. Change in zonal mean concentration of chemical species at 85°S latitude and 20 km altitude as a function of time in the case of SD-control (a, d) and SD-PSI (b, e). Difference between the SD-PSI and SD-control cases (c, f). Concentration of chlorine species (a, b, c) and nitrogen species (d, e, f).

and is converted mostly into Cl_2, as shown by reactions R1 and R3. Figure 1d depicts a strong denitrification of the lower stratosphere during June.

In the presence of solar radiation, Cl_2 is immediately photolyzed

$$Cl_2 + h\nu \rightarrow 2Cl \tag{R4}$$

and reactive chlorine (i.e., $ClOx = Cl + ClO + 2Cl_2O_2$) is produced, with the maximum mixing ratio of approximately 2.0 ppbv in September. The major ozone destruction mechanism is provided in the following catalytic cycle introduced by *Molina and Molina* [1987]

$$Cl + O_3 \rightarrow ClO + O_2 \tag{R5}$$

$$ClO + ClO + M \rightarrow Cl_2O_2 + M \tag{R6}$$

$$Cl_2O_2 + h\nu \rightarrow Cl + ClO_2 \tag{R7}$$

$$ClO_2 + M \rightarrow Cl + O_2 + M \tag{R8}$$

$$Net : 2O_3 \rightarrow 3O_2 \tag{R9}$$
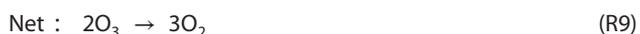
As a result of this efficient destruction mechanism, the model produces an ozone hole in Antarctica during September and October, with a minimum ozone zonal mean total column concentration of 142 DU ranging 84°S–87°S latitude (Figure 2a). This value is somewhat higher than 124 DU; the OMI observed minimum value of the ozone zonal mean total column concentration ranging 85°S–86°S in 2005 [*NASA*, 2014] (green line, Figure 2a). Later in the year, the temperature increases and PSCs disappear. At the same time, the rapid conversion of Cl atoms with methane molecules produces large concentrations of HCl (overshoot seen in Figure 1a). The conversion of ClO to $ClONO_2$ is considerably slower in an atmosphere that has been denitrified (low concentrations of NO_2). The concentrations of $ClONO_2$ and HCl reach their pre-winter values of about 0.4 and 1.4 ppbv, respectively, only in early January (Figure 1a).

3.3. Effect of Ice Injection in the Lower Stratosphere by SD-WACCM

In additional simulations in which temperature and dynamics are specified, ice particles are injected to the lower stratosphere. We denote by PSI, the ice particles that are supplied as part of the geo-engineering action. The saturated vapor pressure of ice, P_{ice} (Pa), is calculated as a function of temperature, T (K), according to the formula of *Sonntag* [1990]

$$\ln P_{ice} = -6024.5282T^{-1} + 29.32707 + 1.0613868 \times 10^{-2}T - 1.3198825 \times 10^{-5}T^2 - 0.49382577 \ln T \tag{16}$$

In the temperature range of 195–210 K, representative of the Antarctic lower stratosphere, the resulting value of P_{ice} ranges from 7.40×10^{-2} to 7.01×10^{-1} Pa. This implies that 2.75×10^{13} to 2.42×10^{14} molecules/cm^3 of water are necessary to produce saturation in this temperature range. Ice particles can exist if the concentration is higher than the above value. Therefore, in order to represent PSI in the model, ice was added with a concentration of 3.0×10^{14} molecule/cm^3 in the prescribed spatial region.

The size of PSI particles is thought to be one of the most important parameters for our problem. The first reason is that the surface area of PSI, proportional to the radius squared, affects the rate of heterogeneous chemical reactions. The second reason is that the terminal velocity of PSI sedimentation, which is related to HCl removal from the stratosphere by sedimentation, is a strong function of the particle's radius. When the size of ice particles is small, the surface area density of PSI becomes large, and degradation of ozone is accelerated. If the particle size is large, the surface area density of PSI is low, and PSI particles are rapidly sedimented from the stratosphere. Under these conditions, the rate of heterogeneous reactions on PSI (i.e., chlorine activation) becomes small, and HCl is efficiently removed. In this case, HCl is removed from the lower stratosphere without degradation of ozone. The problem is slightly more complicated by the fact that large particles also contribute to the denitrification of the atmosphere, and hence exacerbate the ozone destruction by chlorine. The resulting net effect can be assessed by examining the results of the model simulations as described below.

To assess how the size of the injected ice particles influences these different processes, six simulations were performed for a period of 1 month. An objective was to determine the size of PSI that would lead to the optimal removal rate of HCl. The radius of PSI was set at 1, 4, 10, 40, 100, and 400 μm, respectively. With these radii, the terminal velocity (falling speed) was equal to 0.059, 0.24, 1.5, 20, 100, and 400 cm/s, respectively (Table 1), on the basis of the study by *Müller and Peter* [1992]. In this initial first-order study, these values were used at all altitudes in the lower stratosphere. PSI was supplied from 24 to 240 hPa of altitude at latitudes ranging from 70°S to 90°S during May 2–30. The total amount of ClOy (= Cl + ClO, +HCl + $ClONO_2$ + OClO + 2 Cl_2 + 2 Cl_2O_2 + HOCl + BrCl), HCl in ice, and CFC12 was calculated for the conditions encountered in the Antarctic stratosphere, that is, all longitudes, latitude 60°S–90°S, and altitude 2–270 hPa. The difference of the total amount of ClOy, HCl in ice, and CFC12 from May 1 to May 31 is denoted ΔClOy, ΔHCl_ice, and ΔCFC12, respectively. Figure 3 shows the effect of the PSI radius on the amount of HCl removed, which was obtained by deriving −(ΔClOy + ΔHCl_ice), because −ΔClOy provides the amount of HCl taken up in the PSI and −ΔHCl_ice is a measure of the HCl that does not sediment. When no PSI were added to the stratosphere (SD-control case), the total amount of removed HCl was −0.06 Gmol, which means that the total amount of HCl has slightly increased. When PSI were injected with a radius of 1 μm, 0.74 Gmol of HCl was accumulated, because the terminal velocity is very small and PSI, which take up HCl, sediment slowly and stay in the stratosphere for longer time. The amount of HCl removed increased with
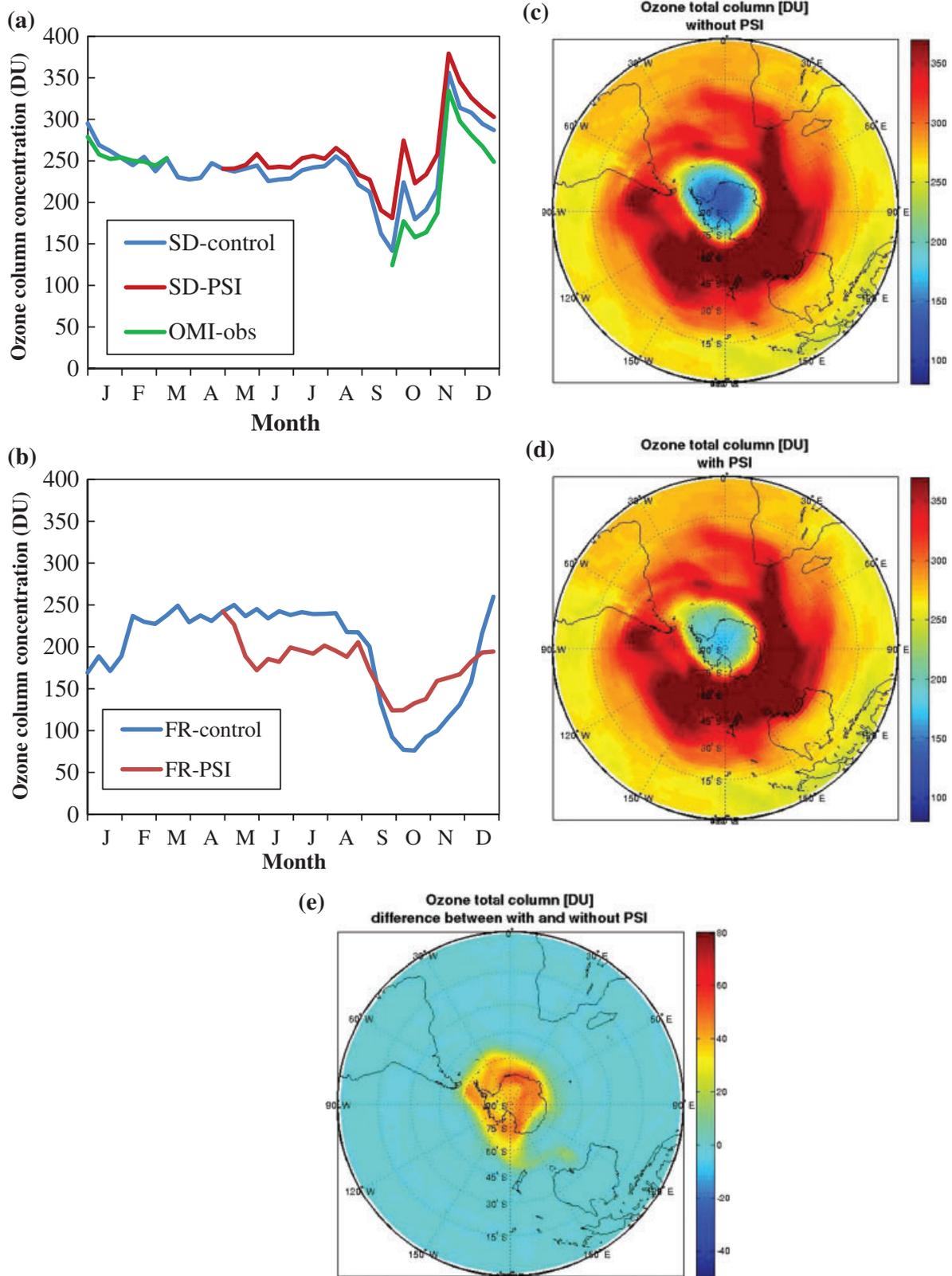
Figure 2. Total column concentration of ozone (DU). Annual change in the ozone zonal mean total column concentration at 85°S latitude without PSI (control) and with PSI in the cases of SD-WACCM (a) and FR-WACCM (b). Distribution of ozone on 28 September for the SD-control case (c), SD-PSI case (d), and difference between these two cases (e).

Table 1. Effect of Particle Size of PSI[a] on the Amount of Cl Species in the Case of FR-WACCM

Radius (µm)	Terminal Velocity (cm/s)	ΔClOy[b] (Gmol)	ΔHCl in Ice[b] (Gmol)	HCl Removed[c] (Gmol)	ΔCFC12[b] (Gmol)
1	0.059	−1.986	2.653	−0.667	0.093
4	0.24	−1.799	1.415	0.385	0.100
10	1.5	−1.723	0.055	1.669	0.104
40	20	−1.548	0.002	1.545	0.110
100	100	−1.351	0.000	1.350	0.116
400	400	−1.142	0.002	1.140	0.129
No PSI	−	−0.140	0.002	0.138	0.022

[a]PSI supplying condition: Altitude range is 24–240 hPa, latitude range is 70°S–90°S in all longitudes, during May 2–30.
[b]Difference May 31 − May 1.
[c]HCl removed = −(ΔClOy + ΔHCl in ice).

the particle's size for radii until 10 µm. In the case of 10 µm, terminal velocity is 1.5 cm/s (13 km/10 day), which means it sediments from the stratosphere to the troposphere for around 10 days. For large particle size (up to 400 µm in our simulations), the rate of HCl removal gradually decreased with the radius, because the surface area density of ice decreases with radius, which means dissolution of HCl also decreases. It is found that the particle size of 10–100 µm is desirable to remove HCl. The particle size of 40 µm was used for further numerical experiments, in which a total removal of HCl of 0.69 Gmol was obtained. This condition is defined as the SD-PSI case.

Figures 1b and 1e show the volume mixing ratio of several chemical species near 85°S latitude at 20 km altitude calculated in the SD-PSI case, and Figures 1c and 1f show the difference of the concentrations between the SD-PSI case and the SD-control case. As HCl was quickly removed in early May and kept to a very low level until middle September, HOCl, which could not react with HCl to produce Cl_2, exhibited higher concentration values from May to September, and Cl_2 exhibited smaller values than that in the SD-control case. The density of active ClOx species, such as Cl, ClO, and Cl_2O_2, was considerably lower than that in the SD-control case during September. The nitrogen compounds, HNO_3 and NOx, exhibit similar change as compared to the values shown in Figure 1b. However, denitrification of the lower stratosphere started in May because of supplied ice particles.

Figure 2a shows the annual change in the total column concentration of ozone around 85°S latitude for both SD cases under consideration. The ozone column concentration becomes smallest in late September in both the simulations. The smallest value is 142 DU in the SD-control case, and 181 DU in the SD-PSI case. The total ozone column concentration on September 30 (at the time close to the ozone minimum) was calculated in
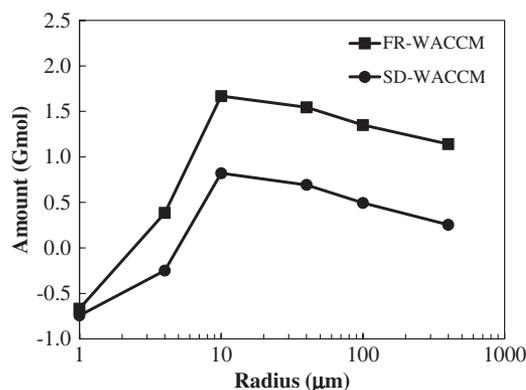
Figure 3. Effect of particle size of PSI on HCl removal in the cases of SD-WACCM and FR-WACCM. The value shown is difference between 31 May and 1 May. PSI was supplied during the period May 2–30 in the altitude range 10.1–26.0 km and in the latitude range 70°S–90°S. The water concentration is 3.0×10^{14} molecule/cm^3.

both the cases as shown in Figures 2c and 2d, respectively. The depth of the ozone hole is substantially reduced as a result of the PSI injection (40 μm radius) in the SD-PSI case. As expected, no major change is noticed outside the Antarctic polar region because, in this particular model case, no potential dynamical feedback was considered. Figure 2e shows the difference of ozone column concentration between the SD-PSI and the SD-control cases. In the Antarctic, the column ozone concentration is 30–55 DU higher in the SD-PSI case, compared to the SD-control case.

3.4. Model Results by FR-WACCM

The simulations mentioned above were performed using SD-WACCM, in which temperatures and the atmospheric dynamics were provided as external data. In this configuration, tracers such as ozone do not feedback on atmospheric dynamics. In the real situations, however, supplying ice will affect not only the chemical composition of the stratosphere but also the heating rates, temperature, and atmospheric dynamics. The second model configuration, FR-WACCM, was therefore used to assess the importance of feedback effects due to dynamical changes.

Figure 2b shows the annual evolution of the total column concentration of ozone around 85°S latitude simulated by FR-WACCM. The smallest value of ozone column concentration is 76 DU in middle October without supplying ice (FR-control case). This very small value arises from the fact that the temperature of the Antarctic lower stratosphere derived by FR-WACCM is very low (i.e., typically 5–10 K colder than in the case of SD-WACCM). With the very low temperatures determined in this version of the model, the breakup time of the Antarctic polar vortex is delayed compared to that in SD-WACCM and, accordingly, the total ozone in November is much lower than that in SD-WACCM. Thus, we will not further discuss in this paper the simulations performed for November and December with FR-WACCM.

To assess the response of the atmosphere to the injection of PSI, we supply the particles again during the entire month of May. When PSI (40 μm radius) was supplied (FR-PSI case), the smallest value of the ozone column concentration was found to be 124 DU in late September, which is about 50 DU higher than that in the FR-control case. A decrease in the ozone column concentration was simulated in May in the FR-PSI case, which was not observed in the SD-PSI case. The reason for this difference is the following: When PSI is supplied, the long-wave heating rate increases (QRL, Figure 4b), where ice exists (H2O_cond, Figure 4a). The temperature increases around 240 hPa and decreases around 20 hPa around 70°S–90°S (delta T, Figure 4d). This warming causes upward movement of air between these levels as shown by the change in diabatic motions (Wd, Figure 4c). This is confirmed by the distribution change of long-lived trace gases, such as CFC-12. The mixing ratio of CFC-12 decreases with height as shown in Figure 5a. The model shows that, in response to PSI injection, a net transport of CFC-12 occurs from the latitude 30°S–60°S around 100 hPa toward latitude 70°S–90°S around 10–100 hPa (delta CFC12, Figure 4e). Similarly, air masses with low ozone mixing ratio rise from the lower stratosphere near the tropopause (Figure 5b) and are diluted around 20–120 hPa in the Antarctic stratosphere (delta O3, Figure 4f). The change in the ozone distribution, however, cannot be explained only by changes in the circulation because ozone is reactive species, and its concentration is also affected by chemical reactions. As a result of these different processes, the total ozone column concentration decreased in latitude from 70°S to 90°S.

In order to confirm that distribution change of ozone is caused by the circulation, the concentration of CFC-12, and ozone in the case of SD-PSI is shown in Figure 5. As the data of temperature and dynamics was externally supplied in the case of SD-WACCM, described in Section 3.1, the circulation did not change when supplying PSI. As a result, the concentration of CFC-12 did not increase but slightly decreased over the Antarctic (Figure 5c), and the distribution change of ozone is similar to that in the FR-PSI case, except in the area around 20–100 hPa over the Antarctic (Figure 5d). This shows that the decrease of ozone concentration in this area found in the FR-PSI case is caused by circulation changes.

As shown in Figure 2b, ozone column concentration remains almost constant from June to August because of the near absence of light during the winter period. The intensity of UV-B is week during winter, and harmful effects on living organisms would be small although the ozone column concentration is smaller in the FR-PSI case than that in the FR-control case. The model simulations suggest therefore that ozone depletion could be substantially reduced by supplying ice to the lower stratosphere in May, before HCl is activated on PSCs.
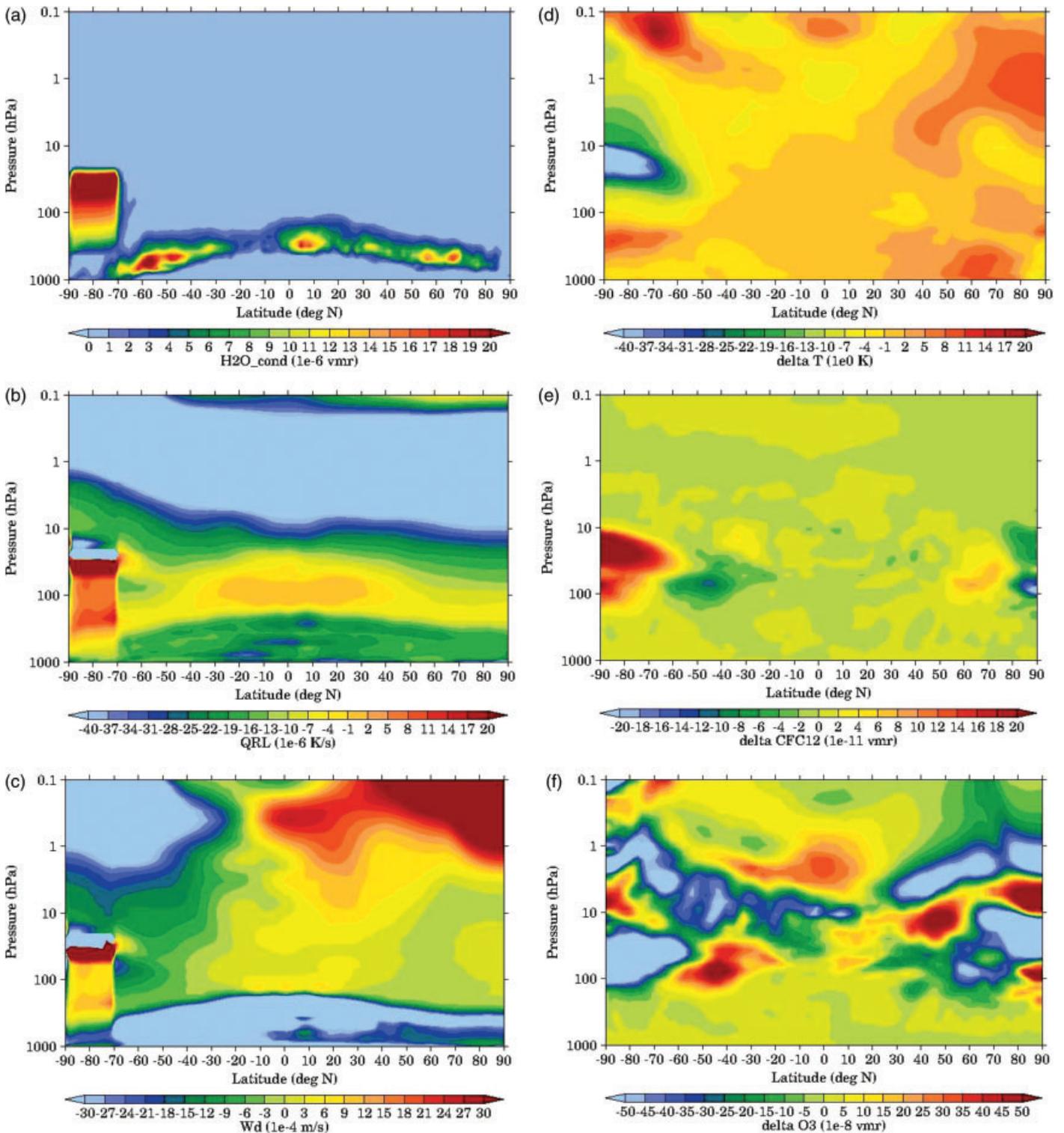
Figure 4. Zonal mean of parameters in the case of FR-PSI. Ice mixing ratio (a), long-wave heating rate (QRL) (b), and vertical velocity of diabatic circulation (Wd) (c) on May 31. Difference between May 31 and May 1 of temperature (d), mixing ratio of CFC-12 (e), and mixing ratio of ozone (f).
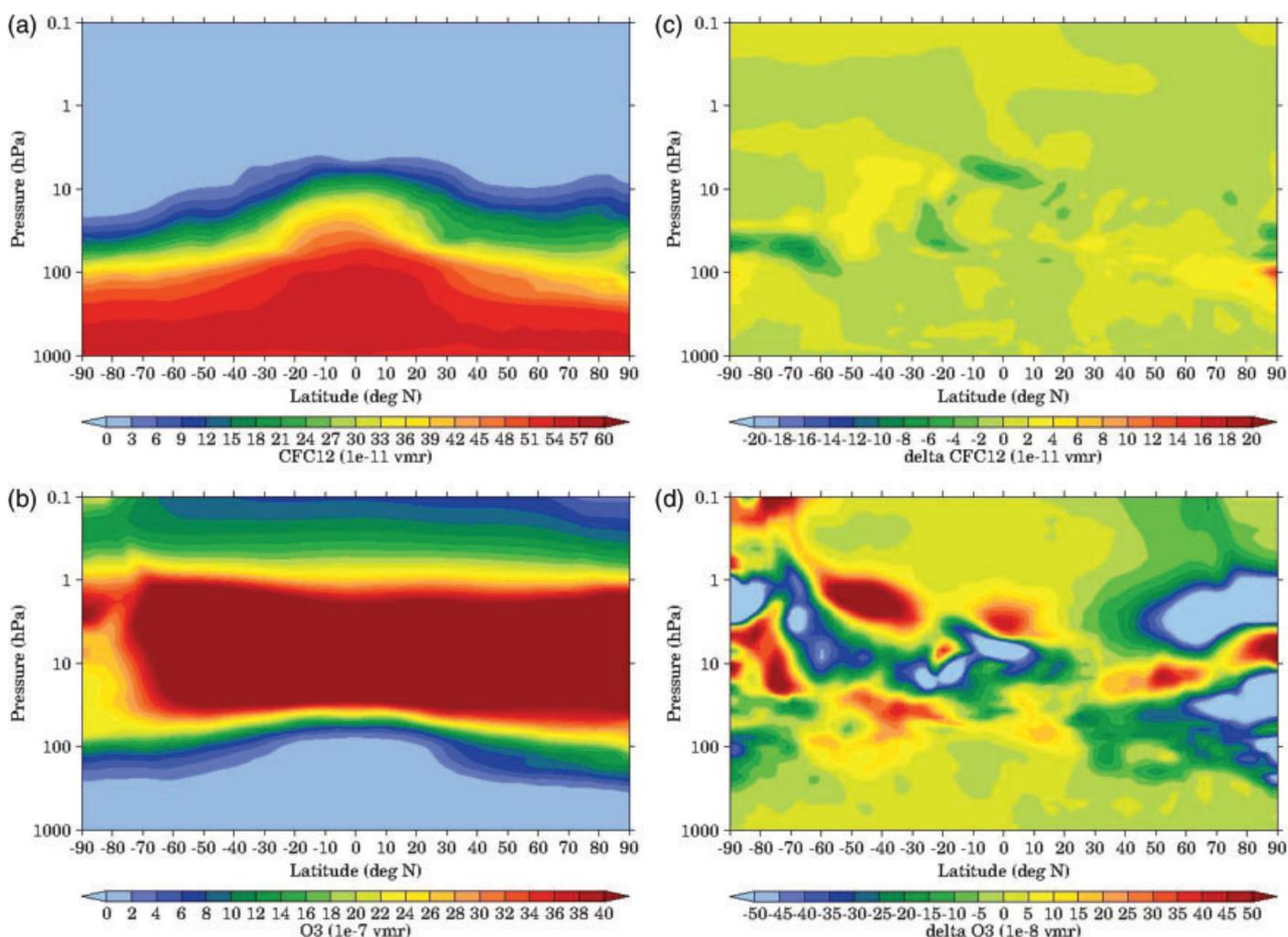
Figure 5. Zonal mean of parameters in the case of SD-PSI. Mixing ratio of CFC-12 (a) and mixing ratio of ozone (b) on May 1. Difference between May 31 and May 1 of mixing ratio of CFC-12 (c) and mixing ratio of ozone (d).

3.5. Suitable Conditions for Supplying Ice Derived From FR-WACCM

The effect of radius, altitude, latitude, period, and amount of injected PSI on HCl removal was investigated by performing five different model experiments. The case of FR-PSI was used as the base condition, in which PSI (radius 40 μm) was supplied at the concentration of 3.0×10^{14} molecule/cm^3 from 24 to 240 hPa of altitude in the latitude range between 70°S and 90°S during May 2–30.

Table 1 shows the effect of the PSI radius (1, 4, 10, 40, 100, and 400 μm) on the amount of HCl removed, which was obtained again by deriving $-(\Delta ClOy + \Delta HCl\_ice)$. The amount of removed HCl is 0.138 Gmol without PSI added to the stratosphere (FR-control case). The values of HCl removed are also plotted in Figure 3. The effect of radius in the FR-PSI case is similar to the effects obtained in the SD-PSI case. However, the amount of HCl removed is about 0.85 Gmol higher than in the SD-PSI case. This is attributed to the dilution by the circulation change, because the higher the pressure level is, the lower the mixing ratio of HCl is. The value of ΔCFC12 increased with increasing radius, because the mixing ratio of CFC-12 is higher in higher pressure level. Numerical experiments suggest that particle sizes of 10–100 μm are desirable to remove HCl efficiently. As in reality, PSI is characterized by a spectrum of particle sizes, a mean particle size of 40 μm was used for further experiments; in this case the removal of HCl is estimated to be 1.55 Gmol.

When PSI was supplied in the altitudes ranging from 10.1 to 15.3, 20.8, 26.0, and 30.4 km, the amount of removed HCl was 0.50, 1.14, 1.55, and 1.44 Gmol, respectively (Table 2). Although it is expected that larger

Table 2. Effect of Altitude at Which PSI Is Supplied[a] on the Amount of Cl Species in the Case of FR-WACCM

Altitude Range (km)	Pressure Range (hPa)	ΔClOy[b] (Gmol)	ΔHCl in Ice[b](Gmol)	HCl Removed[c] (Gmol)	ΔCFC12[b] (Gmol)
10.1 – 15.3	113 – 240	−0.510	0.006	0.504	0.009
10.1 – 20.8	52 – 240	−1.146	0.003	1.144	0.083
10.1 – 26.0	24 – 240	−1.548	0.002	1.545	0.110
10.1 – 30.4	13 – 240	−1.448	0.005	1.443	0.067
15.3 – 20.8	52 – 113	−0.803	0.004	0.799	0.067
15.3 – 26.0	24 – 113	−1.052	0.016	1.035	0.075
15.3 – 30.4	13 – 113	−0.972	0.014	0.958	0.056
20.8 – 26.0	24 – 52	−0.512	0.024	0.488	0.040
20.8 – 30.4	13 – 52	−0.481	0.024	0.457	0.032

[a]PSI supplying condition: Radius 40 μm, latitude range is 70°S – 90°S in all longitudes, during May 2 – 30.
[b]Difference May 31 − May 1.
[c]HCl removed = −(ΔClOy + ΔHCl in ice).

amounts of HCl would be removed when the PSI injection occurs in a wider altitude range, the removal is largest when the injection takes place between 10.1 and 26.0 km. The fact that the value of ΔCFC12 is higher than that in the entire 10.1 – 30.4 km layer is explained by combining the effects of sedimentation of HCl and dilution of HCl by the upward movement of atmosphere. Supplying PSI only to the lower stratosphere in the 10.1 – 15.3 km or in the 15.3 – 20.8 km layer was not effective, because large concentration of HCl exists at higher altitudes. Supplying ice only to higher levels at 20.8 – 26.0 km or 30.4 km has limited effects on HCl removal, because the ice injected at these heights evaporates during sedimentation process. The highest removal rate was obtained when PSI is supplied between 10.1 and 26.0 km. Therefore, we selected this altitude range for further simulations.

When the latitude range for PSI supply was changed from 65°S, 70°S, 75°S, and 80°S to 90°S, the amount of HCl removed was 1.79, 1.55, 1.25, and 0.97 Gmol, respectively (Table 3). The wider the latitude range was, the larger the removal of HCl was. Efficient removal is found for the 70°S – 80°S latitudinal belt as much as for 70°S – 90°S area. The smaller area (70°S – 80°S) is therefore suitable for an effective geo-engineering approach.

Table 4 shows the effect on HCl removal for the time period during which PSI is supplied. For these experiments, HCl removal was calculated as difference in HCl mass between May 1 and June 30. When the supply of PSI was limited to a period of 10 days, HCl was most effectively removed when this injection

Table 3. Effect of Latitude at Which PSI Is Supplied[a] on the Amount of Cl Species in the Case of FR-WACCM

Latitude Range (°S)	ΔClOy[b] (Gmol)	ΔHCl in Ice[b] (Gmol)	HCl Removed[c] (Gmol)	ΔCFC12[b] (Gmol)
65 – 90	−1.796	0.006	1.790	0.130
70 – 90	−1.548	0.002	1.545	0.110
75 – 90	−1.254	0.002	1.252	0.104
80 – 90	−0.969	0.002	0.967	0.052
70 – 80	−1.528	0.002	1.526	0.117
75 – 80	−1.003	0.002	1.001	0.039
70 – 75	−1.310	0.003	1.307	0.053
65 – 70	−1.498	0.006	1.492	0.087

[a]PSI supplying condition: Radius 40 μm, altitude range is 24 – 240 hPa, all longitude zones, during May 2 – 30.
[b]Difference May 31 − May 1.
[c]HCl removed = −(ΔClOy + ΔHCl in ice).

Table 4. Effect of Supplying Period of PSI[a] on the Amount of Cl Species in the Case of FR-WACCM

Period	$\Delta ClOy$[b] (Gmol)	ΔHCl in Ice[b] (Gmol)	HCl Removed[c] (Gmol)	$\Delta CFC12$[b] (Gmol)
2–11 May	−1.042	0.001	1.041	0.044
11–20 May	−1.087	0.002	1.085	0.055
21–30 May	−1.242	0.002	1.240	0.084
1–10 June	−1.185	0.001	1.183	0.087
11–20 June	−1.187	0.002	1.186	0.073
20–29 June	−1.129	0.009	1.120	0.046
2–30 May	−1.414	0.000	1.414	0.114
1–29 June	−1.496	0.003	1.493	0.131
2 May to 29 June	−1.608	0.002	1.606	0.146

[a]PSI supplying condition: Radius 40 μm, altitude range is 24–240 hPa, latitude range is 70°S–90°S in all longitudes.
[b]Difference June 30 − May 1.
[c]HCl removed = −($\Delta ClOy$ + ΔHCl in ice).

was taking place in late May. The removal of HCl was also quite efficient when the 10-day injection was shifted to June. The largest removal rate of HCl was obtained when PSI was supplied for two months during May and June.

Table 5 shows the amount of HCl removed for different concentrations of supplied PSI. Effective removal of HCl was obtained when the PSI concentration was in the range from 1.0×10^{14} to 5.0×10^{14} molecule/cm^3. The corresponding amount of water required to effectively reduce HCl poleward of 70°S in the altitude between 10 and 26 km is about 2.5×10^{17} m^3. When the concentration of ice supplied to produce PSI was 3.0×10^{14} molecule/cm^3, the amount of water to be injected was 7.5×10^{37} molecules. Thus, approximately 2.2×10^9 tons of water is necessary to remove HCl from the polar lower stratosphere. This is a considerable amount for which practical methods of injection—not discussed in the present paper—need to be developed. By comparison, a cloud system which produces rain in an area of 100 km × 100 km at 220 mm (precipitation) contains this amount of water.

In summary, the numerical simulations show that the most suitable condition for removing HCl by supplying ice in the lower stratosphere requires that the radius of the ice particles be 40 μm, the injection altitude 10–26 km, the latitude of 70°S–80°S, the ice concentration of 3.0×10^{14} molecule/cm^3, and period of injection May–July.

Table 5. Effect of Concentration at Which PSI Is Supplied[a] on the Amount of Cl Species in the Case of FR-WACCM

Concentration (molecule/cm^3)	$\Delta ClOy$[b](Gmol)	ΔHCl in Ice[b](Gmol)	HCl Removed[c](Gmol)	$\Delta CFC12$[b](Gmol)
0.5×10^{14}	−1.098	0.002	1.096	0.029
1.0×10^{14}	−1.417	0.002	1.416	0.100
2.0×10^{14}	−1.471	0.002	1.468	0.100
3.0×10^{14}	−1.548	0.002	1.545	0.110
4.0×10^{14}	−1.597	0.005	1.592	0.112
5.0×10^{14}	−1.554	0.001	1.552	0.102
6.0×10^{14}	−0.954	0.001	0.953	0.117

[a]PSI supplying condition: Radius 40 μm, altitude range is 24–240 hPa, all longitude zones, during 2–30 May.
[b]Difference May 31 − May 1.
[c]HCl removed = −($\Delta ClOy$ + ΔHCl in ice).

4. Conclusions

In this study, it was found that the depth of the ozone hole could be significantly reduced by supplying ice to the Antarctic lower stratosphere in late fall (May) before heterogeneous reactions on the surface of natural PSC particles start to activate chlorine. If a sufficiently large amount of ice is injected under favorable conditions, it should remain during several days as ice, and could provide an uptake mechanism for HCl before the formation of PSCs and the activation of chlorine species, if the size of the particles is sufficiently large and sedimentation is sufficiently fast. Without any action, it will take about 40 years for the Antarctic ozone hole to disappear. During this period, the Antarctic region will continue to be exposed to UV-B, with potential impact on living organisms. The proposed approach, which supplies ice to the stratosphere, is designed to accelerate the recovery of ozone in the Antarctic without generating major side effects. Furthermore, because Antarctic ozone is projected to recover in the coming decades, the changes in tropospheric climate forced by ozone depletion in the last decades, specifically in the southern hemisphere, are likely to be reversed in the 21st century. The recovery of ozone may counteract on the tropospheric circulation change caused by increase of greenhouse gases [*Son et al.*, 2008, 2010; *Gillett and Son*, 2012], and climate may therefore benefit from the proposed geo-engineering approach. It was also found that CFCs were transported upward by supplying ice, so that their atmospheric degradation may be accelerated under the proposed method. Thus, because CFCs are strong greenhouse gases, supplying ice may be useful for mitigation of global warming. The impact of injecting ice in the stratosphere on climate forcing and the related climate response needs to be further investigated, using comprehensive three-dimensional climate-chemistry models and investigate possible influences on the climate system over a long period.

To close, we should emphasize again that this study should be regarded as a first-order model investigation of the response of Antarctic ozone to the injection of water in the lower stratosphere. Some assumptions or simplifications have been made in the model formulation and require more attention in future investigations. For example, the effects of microphysical processes on the injected ice particles, and specifically on their size distribution, were not investigated. Feedbacks on the atmospheric circulation also require more attention in future studies. Finally, the risks resulting from the proposed geo-engineering approach should be estimated. Probably, a major risk is that PSI injection does not remove HCl as effectively as calculated by the model. Some error in the evaporation process of PSI that might result from model biases of temperature and water vapor amount may reduce the removal rate of HCl in the lower stratosphere. If this was the case, the reduction in the ozone depletion would be smaller, and the ozone column could decrease as a result of the injection of PSI. However, no model simulation performed for different assumptions has shown a deepening of the ozone hole. The key for the success of the proposed process is that the removal of HCl takes place before the onset of the chlorine activation by particles.

Appendix A: Parameters for Uptake Coefficients

The parameters used in Equation (5) to calculate the uptake coefficient for gas-phase, Γ_g^X, are shown in Table A1, and the parameters used in Equations (6)–(8) to calculate the uptake coefficient for reaction, Γ_{Ri}^X, are shown in Table A2.

Table A1. Parameters for Calculating the Uptake Coefficient for Gas-Phase

Parameter	Expression	Unit	Comment and Reference
Sh_X	$2 + 0.60\,Re^{1/2}Sc_X^{1/3}$	–	Sherwood number, *Ranz and Marshall* [1952]; *Seinfeld and Pandis* [2006]
Re	$2aU/\nu$	–	Reynolds number
Sc_X	$\nu/D_g{}^X$	–	Schmidt number
ν	μ/ρ	m^2/s	Kinematic viscosity of air
μ	$1.458 \times 10^{-6}T^{3/2}/(T+110.4)$	Ns/m^2	Viscosity of air, Sutherland's formula
ρ	$28.96 \times 10^{-3}P/RT$	kg/m^3	Density of air
P		Pa	Pressure

Table A1. (continued)

Parameter	Expression	Unit	Comment and Reference
T		K	Temperature
R	8.314	J/molK	Gas constant
D_g^X	$\dfrac{6.7\times10^{-8}\,T^{1.83}}{P\left[(T_{c1}/P_{c1})^{1/3}+(T_{c2}/P_{c2})^{1/3}\right]^3}\sqrt{\dfrac{1}{M_1}+\dfrac{1}{M_2}}$	m²/s	Binary diffusion coefficient for gases, *Fujita* [1964]; *Joback and Reid* [1987]
	HCl: $T_{c1}=324.6$ K, $P_{c1}=81.5$ atm, $M_1=36.46$		
	ClONO$_2$: $T_{c1}=635.2$ K, $P_{c1}=62.2$ atm, $M_1=97.46$		
	HOCl: $T_{c1}=500.0$ K, $P_{c1}=73.0$ atm, $M_1=52.46$		
	Air: $T_{c2}=132.5$ K, $P_{c2}=37.2$ atm, $M_2=28.96$		
	Tc, critical temperature; Pc, critical pressure		
	T, temperature (K); P, pressure (atm)		
U	Table 1	m/s	Terminal velocity of PSI particles, *Müller and Peter* [1992]
A	Table 1	m	Radius of PSI particles
$\bar{v}_X$	$\sqrt{8k_B T/m_X\pi}$	m/s	Mean thermal velocity
	k_B, Boltzmann constant; $m_{X,}$ mass of molecule X		

Table A2. Parameters for Calculating the Limiting Uptake Coefficient for Reaction

Parameter	Expression	Unit	Comment and Reference
α_X	HCl: 0.30	–	Surface accommodation coefficient, *Crowley et al.* [2010]
	ClONO$_2$: 0.50		
γ_{gs}^X	ClONO$_2$: 0.24	–	Reactive uptake coefficient, *Crowley et al.* [2010]
	HOCl: 0.22		
θ_{HCl}	$\dfrac{K_{lang}^{HCl}[HCl]_g}{1+K_{lang}^{HCl}[HCl]_g+K_{lang}^{HNO3}[HNO_3]_g}$	–	Fractional surface coverage of HCl, *Fernandez et al.* [2005]
θ_{HNO3}	$\dfrac{K_{lang}^{HNO3}[HNO_3]_g}{1+K_{lang}^{HNO3}[HNO_3]_g}$	–	Fractional surface coverage of HNO$_3$, *Fernandez et al.* [2005]
K_{lang}^X	HCl: $0.0219\exp(2858/T)/N_{max}^{HCl}$	cm³/molecule	Langmuir equilibrium constant, *Crowley et al.* [2010]
	HNO$_3$: $7.5\times10^{-5}\exp(4585/T)/N_{max}^{HNO3}$		
	ClONO$_2$: $1.04\exp(2032/T)/N_{max}^{ClONO2}$		
N_{max}^X	HCl, ClONO$_2$: 3×10^{14}	molecule/cm²	Number density of surface adsorbed species at saturation, *Crowley et al.* [2010]
	HNO$_3$: 2.7×10^{14}		
k_s	5×10^{-17}	cm²/molecules	Surface reaction rate coefficient, *Crowley et al.* [2010]
$[H_2O]_s$	$1\times10^{15}-3N_{max}^{HNO3}\theta_{HNO3}$	molecule/cm²	Surface concentration of H$_2$O, *Crowley et al.* [2010]

References

Aguzzi, A., B. Flückiger, and M. J. Rossi (2003), The nature of the interface and the diffusion coefficient of HCl/ice and HBr/ice in the temperature range 190–205 K, *Phys. Chem. Chem. Phys.*, *5*, 4157–4169, doi:10.1039/b308422c.

Boyce, D. G., M. R. Lewis, and B. Worm (2010), Global phytoplankton decline over the past century, *Nature*, *446*, 591–596.

Brasseur, G. P., and S. Solomon (2005), *Aeronomy of the Middle Atmosphere, Chemistry and Physics of the Stratosphere and Mesosphere*, 3rd revised and enlarged ed., pp., Springer, Dordrecht, Netherlands.

Carslaw, K. S., S. L. Clegg, and P. Brimblecombe (1995), A thermodynamic model of the system HCl-HNO$_3$-H$_2$SO$_4$-H$_2$O including solubilities of HBr, from <200 K to 328 K, *J. Phys. Chem.*, *99*, 11557–11574.

Chubachi, S. (1984), Preliminary result of ozone observation at Syowa Station from February, 1982, to January, 1983, *Mem. Natl. Inst. Polar Res. Spec. Issue Jpn.*, *34*, 13–19.

Cox, R. A., M. A. Fernandez, A. Symington, M. Ullerstamb, and J. P. D. Abbatt (2005), A kinetic model for uptake of HNO$_3$ and HCl on ice in a coated wall flow system, *Phys. Chem. Chem. Phys.*, *7*, 3434–3442, doi:10.1039/b506683b.

Crowley, J. N., M. Ammann, R. A. Cox, R. G. Hynes, M. E. Jenkin, A. Mellouki, M. J. Rossi, J. Troe, and T. J. Wallington (2010), Evaluated kinetic and photochemical data for atmospheric chemistry: Volume V—Heterogeneous reactions on solid substrates, *Atmos. Chem. Phys.*, *10*, 9059–9223, doi:10.5194/acp-10-9059-2010.

Emmons, L. K., et al. (2010), Description and evaluation of the Model for Ozone and Related chemical Tracers, version 4 (MOZART-4), *Geosci. Model Dev.*, *3*, 43–67, doi:10.5194/gmd-3-43-2010.

Eyring, V., et al. (2010), Multi-model assessment of stratospheric ozone return dates and ozone recovery in CCMVal-2 models, *Atmos. Chem. Phys.*, *10*, 9451–9472, doi:10.5194/acp-10-9451-2010.

Farman, J. C., B. G. Gardiner, and J. D. Shanklin (1985), Large losses of total ozone in Antarctic reveal seasonal ClOx/NOx interaction, *Nature*, *315*, 207–210, doi:10.1038/315207a0.

Fernandez, M. A., R. G. Hynes, and R. A. Cox (2005), Kinetics of ClONO$_2$ reactive uptake on ice surfaces at temperatures of the upper troposphere, *J. Phys. Chem. A*, *109*, 9986–9996.

Fujita, S. (1964), Coefficient of diffusion in gaseous systems, *Kagaku-kogaku*, *28*, 251–254.

Gillett, N. P., and S.-W. Son (2012), Impact of polar ozone loss on the troposphere, in *Stratospheric Ozone Depletion and Climate Change*, edited by R. Müller, pp. 190–213, RSC Publishing, Cambridge, U. K.

Huthwelker, T., M. E. Malmström, F. Helleis, G. K. Moortgat, and T. Peter (2004), Kinetics of HCl uptake on ice at 190 and 203 K: Implications for the microphysics of the uptake process, *J. Phys. Chem. A*, *108*, 6302–6318, doi:10.1021/jp0309623.

Hynes, R. J., J. C. Mossinger, and R. A. Cox (2001), The interaction of HCl with water-ice at tropospheric temperatures, *Geophys. Res. Lett.*, *28*, 2827–2830, doi:10.1029/2000GL012706.

Joback, K. G., and R. C. Reid (1987), Estimation of pure-component properties from group-contributions, *Chem. Eng. Commun.*, *57*, 233–243.

Kinnison, D. E., et al. (2007), Sensitivity of chemical tracers to meteorological parameters in the MOZART-3 chemical transport model, *J. Geophys. Res.*, *112*, D20302, doi:10.1029/2006JD007879.

Krieger, U. K., T. Huthwelker, C. Daniel, U. Weers, T. Peter, and W. A. Lanford (2002), Rutherford backscattering to study the near-surface region of volatile liquids and solids, *Science*, *295*, 1048–1050, doi:10.1126/science.1066654.

Kunz, A., L. L. Pan, P. Konopka, D. E. Kinnison, and S. Tilmes (2011), Chemical and dynamical discontinuity at the extratropical tropopause based on START08 and WACCM analysis, *J. Geophys. Res.*, *116*, D24302, doi:10.1029/2011JD016686.

Lamarque, J.-F., et al. (2012), CAM-chem: Description and evaluation of interactive atmospheric chemistry in the Community Earth System Model, *Geosci. Model Dev.*, *5*, 369–411, doi:10.5194/gmd-5-369-2012.

Lin, S.-J. (2004), A "vertically-Lagrangian" finite-volume dynamical core for global atmospheric models, *Mon. Weather Rev.*, *132*, 2293–2307.

Marsh, D. R., M. J. Mills, D. E. Kinnison, J.-F. Lamarque, N. Calvo, and L. M. Polvani (2013), Climate change from 1850 to 2005 simulated in CESM1 (WACCM), *J. Clim.*, *26*(19), 7372–7391, doi:10.1175/JCLI-D-12-00558.1.

McNeill, V. F., F. M. Geiger, T. Loerting, B. L. Trout, L. T. Molina, and M. J. Molina (2007), Interaction of hydrogen chloride with ice surfaces: The effects of grain size, surface roughness, and surface disorder, *J. Phys. Chem. A*, *111*, 6274–6284.

Molina, L. T., and M. J. Molina (1987), Production of Cl$_2$O$_2$ from the self-reaction of ClO radical, *J. Phys. Chem.*, *91*, 433–436.

Müller, R., and T. Peter (1992), The numerical modelling of the sedimentation of polar stratospheric cloud particles, *Ber. Bunsen Ges. Phys. Chem.*, *96*(3), 353–361.

Naganobu, M., K. Kutsuwada, Y. Sasai, S. Taguchi, and V. Sieges (1999), Relationships between Antarctic krill (*Euoehausia superba*) variability and westerly fluctuations and ozone depletion in the Antarctic Peninsula area, *J. Geophys. Res.*, *104*(C9), 20651–20665, doi:10.1029/1999JC900136.

NASA (2014), Ozone and air quality, OMI ozone. [Available at http://macuv.gsfc.nasa.gov/OMIOzone.md.]

Neale, R. B., J. Richter, S. Park, P. H. Lauritzen, S. J. Vavrus, P. J. Rasch, and M. Zhang (2013), The mean climate of the Community Atmosphere Model (CAM4) in forced SST and fully coupled experiments, *J. Clim.*, *26*(14), 5150–5168, doi:10.1175/JCLI-D-12-00236.1.

Ranz, W. E., and M. R. Marshall (1952), Evaporation from drops, Part I, *Chem. Eng. Prog.*, *48*, 141–146.

Sander, S. P., J. Abbatt, J. R. Barker, J. B. Burkholder, R. R. Friedl, D. M. Golden, R. E. Huie, C. E. Kolb, M. J. Kurylo, G. K. Moortgat, V. L. Orkin, and P. H. Wine (2011), Chemical kinetics and photochemical data for use in atmospheric studies, evaluation number 17. JPL Publication 10-6, Jet Propulsion Laboratory, Pasadena, Calif. [Available at http://jpldataeval.jpl.nasa.gov.]

Seinfeld, J. H., and S. N. Pandis (2006), *Atmospheric Chemistry and Physics: From Air Pollution to Climate Change*, 2nd ed., pp., Wiley-Interscience, Hoboken, New Jersey.

Solomon, S. (1988), The mystery of the Antarctic Ozone "Hole", *Rev. Geophys.*, *26*(1), 131–148, doi:10.1029/RG026i001p00131.

Solomon, S., R. R. Garcia, F. S. Rowland, and D. J. Wuebbles (1986), On the depletion of Antarctic ozone, *Nature*, *321*, 755–758, doi:10.1038/321755a0.

Son, S.-W., L. M. Polvani, D. W. Waugh, H. Akiyoshi, R. Garcia, D. Kinnison, S. Pawson, E. Rozanov, T. G. Shepherd, and K. Shibata (2008), The impact of stratospheric ozone recovery on the southern hemisphere westerly jet, *Science*, *320*, 1486–1489, doi:10.1126/science.1155939.

Son, S.-W., et al. (2010), Impact of stratospheric ozone on Southern Hemisphere circulation change: A multimodel assessment, *J. Geophys. Res.*, *115*, D00M07, doi:10.1029/2010JD014271.

Sonntag, D. (1990), Important new values of the physical constants of 1986, vapor pressure formulations based on the ITS-90, and psychrometer formulae, *Z. Meteorol.*, *70*, 340–344.

SPARC CCMVal (2010), SPARC report on the evaluation of chemistry climate models, *SPARC Rep. 5*, SPARC, Toronto, Ont., Canada. [Available at http://www.sparc-climate.org/publications/sparc-reports/sparc-report-no5/.]

United Nations Environment Programme (UNEP) (2010), Environmental effects of ozone depletion and its interactions with climate change: 2010 assessment.

Vesala, T., A. U. Hannemann, B. P. Luo, M. Kulmala, and T. Peter (2001), Rigorous treatment of time-dependent trace gas uptake by droplets including bulk diffusion and surface accommodation, *J. Aerosol Sci.*, *32*, 843–860.

Wegner, T., D. E. Kinnison, R. R. Garcia, and S. Solomon (2013), Simulation of polar stratospheric clouds in the specified dynamics version of the Whole Atmosphere Community Climate Model, *J. Geophys. Res.*, *118*, 4991–5002, doi:10.1002/JGRD.50415.

World Meteorological Organization/United Nations Environment Programme (WMO/UNEP) (1989), Scientific assessment of ozone depletion, *Rep. 20*.

World Meteorological Organization/United Nations Environment Programme (WMO/UNEP) (1991), Scientific assessment of ozone depletion, *Rep. 25*.

World Meteorological Organization (WMO) (2007), Global ozone research and monitoring project, *Rep. 50,* World Meteorological Organization.